



HAL
open science

Measurement Quality assessment in urban environments using correlation function distortion metrics

Philippe Brocard, Paul Thevenon, Olivier Julien, Daniel Salós, Mikaël
Mabilleau

► **To cite this version:**

Philippe Brocard, Paul Thevenon, Olivier Julien, Daniel Salós, Mikaël Mabilleau. Measurement Quality assessment in urban environments using correlation function distortion metrics. ION GNSS+ 2015 , Sep 2015, Tampa, United States. hal-01257340

HAL Id: hal-01257340

<https://enac.hal.science/hal-01257340v1>

Submitted on 13 Jun 2016

HAL is a multi-disciplinary open access archive for the deposit and dissemination of scientific research documents, whether they are published or not. The documents may come from teaching and research institutions in France or abroad, or from public or private research centers.

L'archive ouverte pluridisciplinaire **HAL**, est destinée au dépôt et à la diffusion de documents scientifiques de niveau recherche, publiés ou non, émanant des établissements d'enseignement et de recherche français ou étrangers, des laboratoires publics ou privés.

Measurement Quality Assessment in Urban Environments using Correlation Function Distortion Metrics

Philippe Brocard, Paul Thevenon, Olivier Julien, *Ecole Nationale de l'Aviation Civile, France*
Daniel Salos, Mikael Mabillean, *Egis, France*

BIOGRAPHIES

Philippe Brocard graduated from ENAC (the French civil aviation school) with an engineer diploma in 2012. He is currently a PhD student at ENAC and studies signal processing algorithms, sensor fusion and integrity monitoring techniques adapted to the navigation in urban areas. His thesis is funded by GSA (European GNSS Agency), ENAC and Egis Avia.

Paul Thevenon graduated as electronic engineer from Ecole Centrale de Lille in 2004 and obtained in 2007 a research master at ISAE in space telecommunications. In 2010, he obtained a Ph.D. degree in the signal processing laboratory of ENAC in Toulouse, France. From 2010 to 2013, he was employed by CNES, the French space agency, to supervise GNSS research activities and measurement campaigns. Since July 2013, he is employed by ENAC as Assistant Professor. His current activities are GNSS signal processing, GNSS integrity monitoring and hybridization of GNSS with other sensors.

Olivier Julien is the head of the SIGnal processing and NAVigation (SIGNAV) research group of the TELECOM lab of ENAC (French Civil Aviation University), Toulouse, France. His research interests are GNSS receiver design, GNSS multipath and interference mitigation, and interoperability. He received his engineer degree in 2001 in digital communications from ENAC and his PhD in 2005 from the Department of Geomatics Engineering of the University of Calgary, Canada.

Daniel Salós graduated as a telecommunication engineer in 2006 from the University of Saragossa, Spain, and received his PhD in 2012 from the University of Toulouse, France. Since 2007 he has worked on the GNSS field at different organizations like ESA (European Space Agency) and ENAC (French Civil Aviation University). He integrated Egis Avia in 2014 as a navigation engineer, where he carries out activities related to GNSS and in particular aviation applications.

Mikael Mabillean graduated from ENAC (French Civil Aviation School) in August 2006 and has integrated Egis

Avia as CNS project Engineer. He has been involved since 2006 in Galileo standardization activities for Civil Aviation in the frame of the EUROCAE WG 62 and ICAO NSP group. He is also involved in new concept of operation and new system definition through its work on Advanced RAIM and SBAS L1L5 proposition of standard. Since 2009, Mikael has been contributing in an ionosphere study with the objective to assess the impact of ionosphere perturbation on civil aviation applications using GNSS during the upcoming period of high solar activity.

ABSTRACT

Multipath decreases the accuracy of the GNSS positioning by distorting the correlation function. Based on this observation it is possible to detect abnormally large multipath error by monitoring the correlation function. Indeed for the tracking of the code delay, several correlator outputs that correspond to specific locations on the correlation function are observable. Based on the available observables that are combined to form a metric, one can design a test detection to quantize the distortion. The potential metric candidates are selected based on noise resilience considerations. Afterwards, using a simplified correlator output model, two methods are compared for the determination of the detection thresholds. The value of the thresholds is related to the expected Probability of False Alarm. An analytic way to assess the performance of the coherent tests in term of sensitivity is given. The efficiency of the test can be widely improved by smoothing the correlator outputs or the test variable itself. The discussed metrics are implemented on a realistic GNSS tracking simulator processing the Land Mobile Satellite Channel model developed by the DLR. The correlation between the multipath error and the signal to noise ratio (SNR) is well known. Performances of test based on metrics and SNR are finally compared.

INTRODUCTION

Multipath is a well-known phenomenon that affects radio-wave propagation in urban environment. It originates from the interaction of a travelling radio-frequency signal

with urban objects present between the emitting and receiving antenna such as buildings, lamp poles or vehicles. These interactions can be reflection and diffusion by surfaces or diffraction by edges. For the GNSS case, this phenomenon distorts the autocorrelation function which generates a bias on the pseudo-range measurements, which in turn transforms into an error in the position domain. For critical terrestrial applications such as train control or GNSS based electronic toll collection, these biases on the pseudorange may not be acceptable. The use of multipath mitigation techniques such as Narrow Correlator [1], Double-delta techniques [2] or open loop multipath estimation such as A Posteriori Multipath Estimation (APME) [3] can reduce the amplitude of the code tracking error and limit the impact of multipath interference. However important residual biases may still remain in the code delay estimation after the mitigation. For most critical navigation in urban area, the use of an augmentation system is necessary to fulfill the operational integrity requirements. Satellite Based Augmentation Systems (SBAS) and Ground Based Augmentation Systems (GBAS) are not sufficient in urban environment because they can detect Signal in Space (SiS) failures but cannot detect failures due to the receiver environment and in particular multipath. The implementation of a Receiver Autonomous Integrity Monitoring (RAIM) algorithm is necessary to assure the integrity monitoring in these constraint scenarios. However, in urban environment, several pseudoranges may be biased simultaneously and traditional RAIMs algorithms usually assume only a single faulty pseudorange. A possible approach to overcome this limitation consists in focusing on the detection of the failures prior to the integrity monitoring algorithm. In urban areas, pseudorange biases can be observed due to the reception of a Non Line of Sight (NLOS) which leads to an over estimation of the satellite to receiver distance. This phenomenon may be detected at the signal processing level if it involves a loss in term of C/N_0 due to the loss of power during the diffraction/reflection. But this strategy does not detect NLOS that are not associated with important C/N_0 variations. The use of a constant elevation mask for the satellite based on a priori studies is a feasible solution. However, this solution is not optimal in terms of geometry because the actual mask of the environment may be lower at some instant and an unnecessary exclusion of satellites may reduce the quality of the geometry. Techniques based on a fisheye camera mounted on the top of the vehicle could be used in order to detect the elevations of the different buildings and either underweight or provides exclusion flag in order not to consider the satellites that are masked [4]. Other techniques called shadowmatching based on an accurate 3D model of the city can be used and, even if they do not require any additive sensors, a costly calibration step and mapping is required.

This paper focuses on the scenario where the received signal is a linear combination of a Line-of-Sight (LOS) signal and several echoes. The correlation function of the resulting signal is distorted. The aim is to quantize the distortion of the correlation function due to multipath to detect abnormal measurement and exclude them before the integrity monitoring module. The techniques used to quantify the distortion due to multipath are inspired from the research done for the detection of evil waveforms which are anomalies observed on the waveform that model the PRN code [4]. Inspired from this approach, [5] proposed a technique to detect the presence of multipath by monitoring these indicators.

The approach is that of a classical hypothesis testing. A set of hypotheses to test is defined:

- H_0 : no multipath is present
- H_1 : presence of multipath

Distortion metrics which are linear combinations of correlator outputs are used as test variables to detect those distortions. In this paper, existing metrics and a new metric are investigated. A new rigorous approach to calculate the decision thresholds under H_0 and to adjust the Probability of False Alarm (P_{FA}) is proposed and compared to the prior art. The P_{FA} is defined as:

$$P_{FA} = P(H_1|H_0) \quad (1)$$

The theoretical concept of multipath sensitivity under H_1 and associated to a value of Probability of Missed Detection (P_{MD}) is defined and discussed in this paper.

The P_{MD} is defined as:

$$P_{MD} = P(H_0|H_1) \quad (2)$$

Then, the performances of the detection tests are assessed on time series generated by an urban channel model processed by a realistic GNSS receiver simulator.

I. Existing and new metrics

Test Metrics are defined as linear combinations of correlator outputs which enable to quantize the distortion of the autocorrelation function. Usual metrics are detailed in the literature and the two of them that perform the best according to prior art for multipath detection are the so called simple ratio and the differential ratio [5] given in Table 1. Septentrio's APME [6], that performs well for the mitigation of short delay multipath, relies on an estimator which is a simple ratio test that is centered and multiplied by an empirical likelihood factor (0.42). Existing metrics are coherent and therefore can only be used when the carrier is tracked by a Phase Lock Loop (PLL). Let's denote I_X the in-phase correlator output located in X on the correlation function.

Type of Test	Expression
Simple Ratio Tests (M_1)	$\frac{I_X}{I_Y}$
Differential Ratio Tests (M_2)	$\frac{I_X - I_Y}{I_Z}$
Non Coherent Simple Ratio Tests (M_3)	$\frac{I_X^2 + Q_X^2}{I_Y^2 + Q_Y^2}$

Table 1 Metrics of interest

In urban environments, the tracking of the carrier phase by a PLL is less robust than the tracking of the carrier frequency by a Frequency Locked Loop (FLL). However, tracking the frequency leads to a bias on the carrier phase estimate. If this bias is close to $\pi/2$, the useful signal at the in phase correlator output is dominated by thermal noise and computing the ratio between correlator outputs becomes meaningless. Non coherent metrics are proposed in this article because they are compatible with the use of a FLL. The drawback of such metric is the difficulty to accurately characterize its distribution. Coherent metrics will be studied in Chapter II, while non-coherent metrics will be studied in Chapter III.

II. Determination of the detection thresholds for coherent metrics

In this chapter, H_0 holds which means that the receiver is only affected by thermal noise. The general correlator output model at the k^{th} integration index when assuming a linear variation of the phase tracking error during the integration interval is the following:

$$I_X(k) = \sqrt{\frac{C}{2}} d(k) K_{cc}(X + \varepsilon_\tau) \cos(\varepsilon_\varphi) \text{sinc}(\pi \varepsilon_f T_i) + n_X(k) \quad (3)$$

Where

- X is the location of the correlator in chip
- C is the power of the carrier
- $d(k)$ is the data component
- K_{cc} is the autocorrelation function of the PRN filtered by the front end
- ε_τ , ε_φ and ε_f are respectively the delay, phase and Doppler estimation error by the tracking loops
- T_i is the integration duration
- n_X is the thermal noise

In this study the tracking is assumed to be sufficiently precise to neglect ε_τ , ε_φ and ε_f in the nominal case (i.e. Multipath free). This assumption is valid when the carrier is tracked by a PLL. The data are also not considered in the model as they have no impact when the correlator outputs are normalized by another correlator output

corresponding to the same integration index. The simplified correlator output model becomes:

$$I_X(k) = \sqrt{\frac{C}{2}} K_{cc}(X) + n_X(k) \quad (4)$$

The expression of the noise variance at the correlator output is $N_0/(4T_{int})$.

Therefore the reduced in phase correlator output is such that $I_X \sim \mathcal{N}(\mu_X, \sigma_X^2)$ with:

- $\mu_X = \sqrt{2 C/N_0 T_i} \cdot K_{cc}(X)$
- $\sigma_X^2 = 1$
- The covariance between two correlator outputs in X and Y is $\text{cov}(n_X n_Y) = E[n_X n_Y] = K_{cc}(Y - X)$

The objective is now to establish the confidence interval of the metric so that the receiver decide whether it is under H_0 or H_1 . In this subsection we study two different methods for the determination of the thresholds.

Gaussianity assumption

The first method which is the one proposed in [5] assumes that the metrics (Simple Ratio Tests and Differential Ratio Tests) follow Gaussian distributions. Let's denote M an arbitrary metric among the coherent ones, it is assumed that $M \sim \mathcal{N}(\mu_M, \sigma_M^2)$. Therefore the interval of confidence for the metrics is the interval $[\mu_M - m_{exp} \sigma_M; \mu_M + m_{exp} \sigma_M]$ where m_{exp} is an expansion factor that can be adjusted to set the desired P_{FA} . The relation between this factor and the P_{FA} can be obtained with standard tables of Gaussian tails. However the ratio of two Gaussians asymptotically tends to a Gaussian when μ_M/σ_M tends to infinity. This assumption may be relevant in the operating conditions of [5] because the integration time is sufficiently high (1000 ms) and C/N_0 values simulated are high (40/45 dB-Hz). In a standard GNSS receiver the integration time is much shorter (20 ms for GPS L1 C/A at best with data bit synchronization assumed). Moreover C/N_0 can be lower than the range of value tested in the prior art in a challenging environment. For each coherent metric, the bounds of the confidence interval are given in Table 2, and the calculations to obtain them are given in appendix I.

Type of Test	Characteristics of the distribution	
	μ_M	σ_M
Simple Ratio Tests (M_1)	$\frac{\mu_X}{\mu_Y}$	$\frac{\mu_X}{\mu_Y} \sqrt{\left(\frac{\sigma_X^2}{\mu_X^2} + \frac{\sigma_Y^2}{\mu_Y^2} - 2 \frac{\text{cov}_{XY}}{\mu_X \mu_Y}\right)}$
Differential Ratio Tests (M_2)	$\frac{\mu_X - \mu_Y}{\mu_Z}$	$\left(\frac{\mu_X - \mu_Y}{\mu_Z}\right) \sqrt{\frac{\sigma_X^2}{\mu_Z^2} + \frac{\sigma_Y^2 + \sigma_Z^2 - 2\text{cov}_{XY}}{(\mu_X - \mu_Y)^2} + \frac{2\text{cov}_{ZX} - \text{cov}_{ZY}}{\mu_Z(\mu_X - \mu_Y)}}$

Table 2 Thresholds obtained with gaussianity assumption

Proposed method

The approach which is proposed in this paper does not assume any Gaussianity aspect of the metric and then the obtained threshold can be applied to receivers using standard integration time. The Geary-Hinkley transformation [7] [8] makes it possible to form a new random variable that is Gaussian when applied to a ratio of two correlated non central Gaussian variables. If $I_X \sim \mathcal{N}(\mu_X, \sigma_X^2)$ and $I_Y \sim \mathcal{N}(\mu_Y, \sigma_Y^2)$ with a covariance cov_{XY} , then the expression of the Geary-Hinkley transform applied to $M = \frac{I_X}{I_Y}$ is the following:

$$T = \frac{\mu_Y M - \mu_X}{\sqrt{\sigma_Y^2 M^2 - 2cov_{XY} M + \sigma_X^2}} \quad (5)$$

Where $T \sim \mathcal{N}(0,1)$ provided that the denominator is unlikely to assume negative values.

The next step for the thresholds determination is to set the desired P_{FA} on the transformed variable T . Then simply deduces the thresholds of the metrics. Let m_{exp} be the expansion factor corresponding to the expected P_{FA} , the thresholds for M are the roots of the associated second degree equation. For every metrics and the thresholds obtained are given in Table 3.

The validity of the thresholds is directly derived from the validity of the Geary-Hinkley transformation which is $\mu_Y \geq m_{exp} \sigma_Y$. By replacing μ_Y and σ_Y by their expressions, the domain of validity corresponds to:

$$C/N_0 \geq \frac{1}{2T_{int}} \left(\frac{m_{exp}}{K_{cc}(Y)} \right)^2 \quad (6)$$

Type of Test Metric	Thresholds
Simple Ratio Tests (general expression of the bounds)	$\text{Lower bound} = \frac{-(-2\mu_X\mu_Y + 2m_{exp}^2 cov_{XY}) - \sqrt{(-2\mu_X\mu_Y + 2m_{exp}^2 cov_{XY})^2 - 4(\mu_Y^2 - m_{exp}^2 \sigma_Y^2)(\mu_X^2 - m_{exp}^2 \sigma_X^2)}}{2(\mu_Y^2 - m_{exp}^2 \sigma_Y^2)}$ $\text{Upper bound} = \frac{-(-2\mu_X\mu_Y + 2m_{exp}^2 cov_{XY}) + \sqrt{(-2\mu_X\mu_Y + 2m_{exp}^2 cov_{XY})^2 - 4(\mu_Y^2 - m_{exp}^2 \sigma_Y^2)(\mu_X^2 - m_{exp}^2 \sigma_X^2)}}{2(\mu_Y^2 - m_{exp}^2 \sigma_Y^2)}$
Differential Ratio Tests	<p>Substitute X by N, and Y by Z in the general expression, where:</p> $\mu_N = \mu_X - \mu_Y$ $\sigma_N = \sqrt{\sigma_X^2 + \sigma_Y^2 - 2cov_{XY}}$ $cov_{N,Z} = cov_{XZ} - cov_{YZ}$

Table 3 Thresholds without gaussianity assumption

Constraints on the metric candidates

The most promising test metrics have been identified for GPS signals in [5] based on the ratio of the metric's envelope over noise level. Most of these candidates are not relevant for the Galileo signals. They are highly noise sensitive because of the division by noisy correlators. Indeed the slope of the correlation function is higher for BOC signals: 3 in the main peak for BOC(1,1), and $(53 \pm 2\sqrt{10})/11 \approx 5.4$ in the main peak for CBOC(6,1,1/11, \pm), which means that the range of relevant locations for the correlator at the denominator is thinner than for BPSK. This intuitive assumption is well illustrated by the domain of validity of the bounds given in (6). In Figure 1, the lower bound of the validity domain in term of C/N_0 is given as a function of the correlator location for the three modulations with an infinite receiver's front-end bandwidth. The expansion factor is set to a typical value of 3σ which corresponds to a P_{FA} of 0.0027. The operational range of C/N_0 constrains the choice for the normalization correlator. In urban environment where a typical value for the C/N_0 mask is 30 dB-Hz [9] to select the robust measurement in a multi-

GNSS system, for a 3σ expansion factor, the allowed values of Y for BPSK is $[-0.5, 0.5]$ whereas it is $[-0.17, 0.17]$ for BOC(1,1) and CBOC(6,1,1/11).

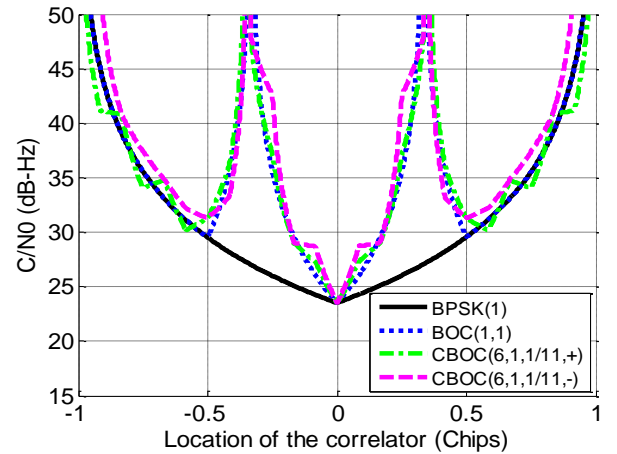


Figure 1 The allowed locations for the correlator used for the normalization of the metric correspond to the area above the curve

As the detectors studied in this paper are likely to be implemented on standard receivers that only process three correlators outputs (prompt, early and late), this will limit the amount of possible combination to form the metric. The validity domain of the BOC imposes the condition of a chip spacing for the DLL lower than 0.34 to normalize the test by either the early or the late correlator output.

Performance assessment of the thresholds

The performances of both thresholds' expression are compared on a typical case of study, in which the receiver may process GPS L1 C/A and Galileo E1 OS. The BW is assumed infinite for simplicity. Three correlator outputs are simulated according to the model, in $X = 0$, $Y = 0.25$ and $Z = 0.125$. Accumulation time is set to 20 ms. The generation of the correlated noise sequences is done by multiplying independent Gaussian random variables by the Cholesky decomposition of the expected noise covariance matrix. The two metrics are calculated. The thresholds are calculated with gaussianity assumption and with the proposed method for a typical range of operating C/N_0 for an expansion factor of 3. The observed P_{FA} is plotted in Figure 2 for each coherent metric on GPS L1 C/A signals.

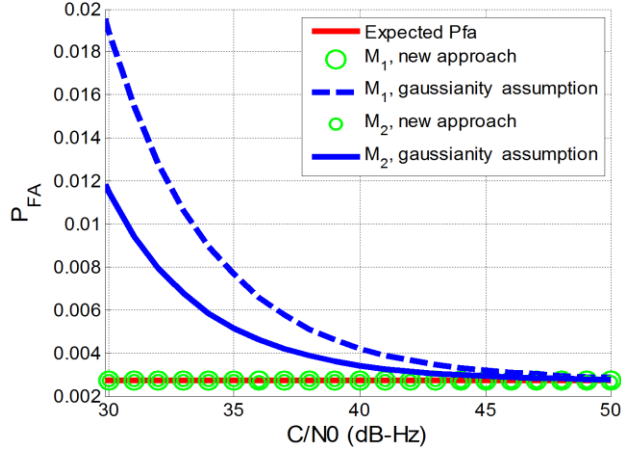


Figure 2 Comparison between the expected P_{FA} (0.0228) and the observed P_{FA}

The Gaussianity of the metric's distribution increases with the C/N_0 . The proposed thresholds enable to set the right P_{FA} , even for low C/N_0 . This observation would be all the more characteristic for lower integration times (typically 1 ms).

III. Determination of the detection thresholds for non-coherent metrics

For non-coherent metrics, the correlator output model is the following:

$$I_X(k) = \sqrt{\frac{C}{2}} d(k) K_{cc}(X) \cos(\varepsilon_\phi) + n_X(k) \quad (7)$$

$$Q_X(k) = \sqrt{\frac{C}{2}} d(k) K_{cc}(X) \sin(\varepsilon_\phi) + n_X(k)$$

The determination of the thresholds for the non-coherent metrics requires the knowledge of its distribution. The term $I_X^2 + Q_X^2$ follows a chi-square distribution with 2 degrees of freedom and a non-centrality parameter $\lambda = 2T_{int} C/N_0 K_{cc}(X)$. The ratio of two non-central uncorrelated χ^2 follows a doubly non-central F distribution [10] [11], with known parameters. However, when considering the correlation between both correlator outputs (X and Y) the distribution is unknown. Therefore, for non-coherent metrics, the thresholds are computed numerically. The interval of non-detection is symmetric and centered on the mean of the metric. The lack of knowledge about the distribution of the metric is the main drawback related to the use of non-coherent metrics.

IV. Theoretical sensitivity

In this subsection, the signal is assumed to be affected by one unique reflection in phase with the direct signal, which is one hypothesis generally assumed for the characterization of multipath mitigation techniques by their multipath envelope although it differs significantly from the urban conditions. The non-coherent metrics are not studied in this section due to the lack of knowledge of their distributions. The general model of the correlator output becomes:

$$I_{X,MP}(k) = \sqrt{\frac{C}{2}} K_{cc}(X) + \frac{1}{\sqrt{SMR}} \sqrt{\frac{C}{2}} K_{cc}(X - \tau) + n_X(k) \quad (8)$$

Where:

- τ is the relative delay of the reflection compared to the direct signal
- SMR is the signal to multipath power ratio

The Gaussian model can be used here with:

$$\begin{aligned} \mu_{X,MP} &= \mu_X + \sqrt{\frac{2C/N_0 T_{int}}{SMR}} K_{cc}(X - \tau) \\ &= \mu_X + \alpha K_{cc}(X - \tau) \end{aligned}$$

The sensitivity is defined as the maximum Signal to Multipath Ratio (SMR) at which the test is positive providing the probability of missed detection (P_{MD}). In this subsection it is assumed that τ is a parameter. Figure 3 illustrate the two scenarios that can occur and can lead to a missed detection. The P_{MD} corresponds to the area (in red) in between the thresholds that were set under H_0 .

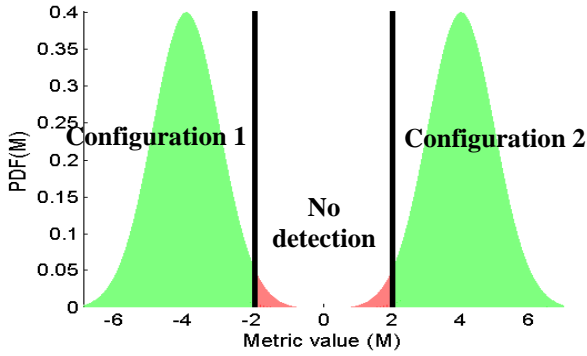


Figure 3 Possible scenarios for the missed detection

The metric affected by multipath have a new distribution, which is unknown. However the multipath only affects the mean of the metric of both numerator and denominator. The calculation of the sensitivity starts from the following statement on the metric:

- Configuration 1:

$$UB_{\exists MP} = LB_{\nexists MP}$$
- Configuration 2:

$$LB_{\exists MP} = UB_{\nexists MP}$$

Where $LB_{\nexists MP}$ and $UB_{\exists MP}$ are respectively the lower bound and upper bound determined in the multipath free

Type of Test Metric	
Simple Ratio Tests (general expression of the sensitivity)	Configuration 1: $\alpha^2\{[UB_{\exists MP}K_{cc}(Y - \tau)]^2 - 2UB_{\exists MP}K_{cc}(Y - \tau)K_{cc}(X - \tau) + K_{cc}(X - \tau)^2\}$ $+ \alpha\{2UB_{\exists MP}^2\mu_Y K_{cc}(Y - \tau) - 2UB_{\exists MP}[\mu_X K_{cc}(Y - \tau) + \mu_Y K_{cc}(X - \tau)] + 2\mu_X K_{cc}(X - \tau)\}$ $+ UB_{\exists MP}^2(\mu_Y^2 - m_{MD}^2\sigma_Y^2) + 2UB_{\exists MP}(-\mu_X\mu_Y + m_{MD}^2cov_{xy}) + \mu_X^2 - m_{MD}^2\sigma_X^2 = 0$
	Configuration 2: $\alpha^2\{[LB_{\nexists MP}K_{cc}(Y - \tau)]^2 - 2LB_{\nexists MP}K_{cc}(Y - \tau)K_{cc}(X - \tau) + K_{cc}(X - \tau)^2\}$ $+ \alpha\{2LB_{\nexists MP}^2\mu_Y K_{cc}(Y - \tau) - 2LB_{\nexists MP}[\mu_X K_{cc}(Y - \tau) + \mu_Y K_{cc}(X - \tau)] + 2\mu_X K_{cc}(X - \tau)\}$ $+ LB_{\nexists MP}^2(\mu_Y^2 - m_{MD}^2\sigma_Y^2) + 2LB_{\nexists MP}(-\mu_X\mu_Y + m_{MD}^2cov_{xy}) + \mu_X^2 - m_{MD}^2\sigma_X^2 = 0$ $SMR = \frac{2C/N_0 T_{int}}{\alpha^2}$
Differential Ratio Tests	Substitute X by N , and Y by Z in the general expression

Table 4 General expression of the theoretical sensitivity

The sensitivity shall be taken into account in the design of the quality monitoring indicator concept. The way to calculate and interpret the sensitivity is given in this study through a realistic example. The C/N_0 is set to 40 dB-Hz, and the metric of interest is M_1 , with $X = 0.25$ and $Y = 0$. The delay of the multipath is arbitrarily set to 0.5 chip. The signal of interest is in this example BPSK(1). This example is also used to validate the obtained results by simulations. The reverse process is done as a validation, where the multipath amplitude is set to the value of the sensitivity for the corresponding P_{FA} . Random draw of the metric value affected to multipath are done, the P_{MD} is then estimated as the proportion of the undetected samples. It can be inferred from Table 5 that the

scenario to set the P_{FA} . The analytic expressions of $UB_{\exists MP}$ and $LB_{\exists MP}$ are obtained using the Geary-Hinkley transformation, by introducing a new expansion factor m_{md} in order to set the P_{MD} . Particular caution must be taken when setting the P_{MD} because as illustrated in Figure 3 the missed detection probability is only due to one of the two Gaussian tail (either left or right). Therefore in order to impose $P_{MD_{true}}$, the expansion factor m_{MD} shall be chosen so that it performs $P_{MD_{bitat}} = 2P_{MD_{true}}$.

Then Configuration 1 is assumed in order to calculate the minimum SMR , which is obtained by solving the second order equation given in Table 4. The validity of the Scenario must be checked afterwards with the following possible indicator:

$$\eta = sign(E[m|\exists MP(SMR, \tau)] - E[m|\nexists MP]) \quad (9)$$

- If η is positive, Scenario 1 is valid.
- If η is negative, Scenario 1 is not valid and the SMR shall be calculated for Scenario 2 with the corresponding equation given in Table 4.

correspondence between the P_{MD} and the sensitivity is well characterized by the theoretical expressions according to the green cells. This table of sensitivity could have been translated into a table of maximum pseudorange error. Indeed, as an example, for a conventional DLL using a narrow correlator to track the GPS L1 C/A signal, the rule of thumb for the envelope of the pseudorange multipath error is:

$$\epsilon_{Multipath} = \frac{1}{\sqrt{SMR}} \cdot \frac{d}{2} \quad (10)$$

Where d is the chip spacing between the early and late correlators of the DLL.

		P_{FA}			
		0.0455	0.0027	6.33e-5	5.73e-7
P_{MD}	0.159	10.7 dB	7.70 dB	5.21 dB	3.00 dB
		0.159	0.159	0.159	0.159
	0.0228	8.20 dB	5.77 dB	3.62 dB	1.67 dB
		0.0228	0.0228	0.0228	0.0228
	0.00135	6.26 dB	4.18 dB	2.29 dB	0.505 dB
		0.00135	0.00135	0.00135	0.00135
	3.17e-5	4.68 dB	2.84 dB	1.13 dB	-0.518 dB
		3.18e-5	3.21e-5	3.21e-5	3.18e-5
	2.87e-7	3.34 dB	1.68 dB	0.105 dB	-1.43 dB
		3.05e-7	3.13e-7	3.03e-7	3.16e-7

Table 5 The white cells represents the sensitivity of the test on GPS L1 C/A for M1 with infinite front end BW. The green cells represent the observed P_{MD} .

For low P_{FA} associated with low P_{MD} , the efficiency of the test in term of sensitivity is low. To improve it, an intuitive idea is to narrow the distribution of the multipath free metric. Multipath has long correlation times compared to the thermal noise which is memoryless (white). Multipath deterministically results in a translation of the distribution of the metric. To narrow the distribution, it is either possible to low pass filter the correlator outputs that are combined to form the metric, or to low pass filter the metric. The smoothing of the correlator outputs is preferred as the new thresholds can easily be calculated when using the proposed approach. Moreover, the filtered denominator is less likely to be null after this filtering step which enable the extension of the domain of validity of the metrics. On the other hand, if the Gaussianity assumption has been used it is more practical to filter the metric instead. The problem relative to such a smoothing is the data term in the correlator output that can be +1 or -1. If an external mean is available to get the data message, it is possible to multiply each correlator by the corresponding sign of the data bit which is known. An alternative is to take the absolute value of each correlator outputs. This step changes the distribution of the correlator output which must then be modelled by a folded normal distribution. This distribution can still be approximated by a Gaussian provided that the correlators are unlikely to assume negative values. This condition is fulfilled if all the correlators used to form the metric are under the conditions of (6). The general model of correlator output becomes:

$$\mu_X = \sqrt{\frac{C/N_0}{2} \frac{C}{B_l}} \cdot K_{cc}(X) \quad (11)$$

$$\sigma_X = 1$$

Where

- B_l is the double-sided equivalent noise bandwidth of the low pass filter

For a noise equivalent bandwidth of 5Hz, the sensitivity is given in Table 6.

		P_{FA}			
		0.0455	0.0027	6.33e-5	5.73e-7
P_{MD}	0.159	21.3 dB	18.7 dB	16.6 dB	14.9 dB
		0.159	0.159	0.159	0.159
	0.0228	18.8 dB	16.7 dB	15.0 dB	13.5 dB
		0.0227	0.0227	0.0228	0.0228
	0.00135	16.9 dB	15.1 dB	13.7 dB	12.4 dB
		0.00134	0.00134	0.00135	0.00135
	3.17e-5	15.3 dB	13.8 dB	12.5 dB	11.3 dB
		3.12e-5	3.15e-5	3.11e-5	3.14e-5
	2.87e-7	13.9 dB	12.6 dB	11.5 dB	10.4 dB
		2.1e-7	1.9e-7	2.3e-7	2.2e-7

Table 6 The white cells represents the sensitivity of the test on GPS L1 C/A for M1 with infinite front end BW with smoothing of the correlator. The green cells represent the observed P_{MD} .

The gain in term of sensitivity obtained by smoothing the correlator outputs with a 5 Hz equivalent noise bandwidth low pass filter is approximately 11 dB in the studied scenario. The domain of validity is also increased thanks to the smoothing of the correlator used for the normalization assuming that the navigation message is known (if the absolute value is calculated, then (6) shall be used):

$$C/N_0 \geq \frac{B_l}{2} \left(\frac{m_{exp}}{K_{cc}(Y)} \right)^2 \quad (12)$$

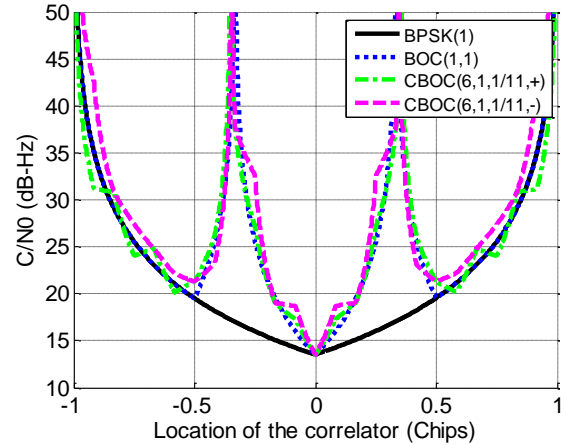


Figure 4 Lower bound of the allowed locations for the correlator used for the normalization of the metric after low pass filtering (5Hz)

V. Performance assessment on urban channel model

The aim of this section is to assess the performances of a test based on the multipath detection metrics to improve the reliability of the pseudoranges estimation in urban environment. The approach consists in coupling the wideband Land Mobile Satellite (LMS) Channel developed by the German Aerospace Center (DLR) [12] which is an open source software, with a realistic GNSS receiver model called geneIQ and developed by ENAC. The LMS is the reference wideband model for the ITU (International Telecommunication Union). A narrowband

model such as the one developed in [13] would not be suitable for this study as it does not generate any distortion on the correlation function which is the phenomenon that is detected in this study. The connection process between the LMS and geneIQ is detailed in [9]. However, we chose to reformulate the test so that it is adapted to urban environment. Indeed in urban environment the receiver is almost always affected by multipath and therefore always under H_1 . The new formulation is based on the definition of a maximum tolerable error (MTE). As an example, the MTE is set to 5 meters. The new hypotheses to test are:

- H_0' : the pseudorange error is lower than the MTE
- H_1' : the pseudorange error is higher than the MTE

The approach used in the initial test consisted in setting the P_{MD} , and then to observe the Sensitivity in dB or in term of pseudorange error. The reformulation consist in setting the Sensitivity in term of pseudorange error, and then to observe the P_{MD} .

Simple ratio metric

As detailed in Chapter IV the implementation of a raw test metrics leads to poor performance in term of sensitivity. This can be illustrated by simulations on the LMS tracked by geneIQ. The channels for satellite elevations of 40, 50, 60, 70, 80° and satellite azimuths of 45 and 90° are concatenated. The LOS is not shadowed for these elevations. Each channel is 1 km long, and the velocity of the vehicle is set to 20 km/h. Thermal noise is added to the correlators with a C/N_0 set to 40 dB-Hz. The receiver used is a wideband (4 MHz) receiver that tracks the L1 C/A signal with a conventional non coherent DLL with a 1 Hz 2nd order loop filter. The Early minus Late spacing of the DLL is set to 0.5 chips. The carrier phase is tracked by a non-coherent *atan* PLL with a 10 Hz 3rd order loop filter. In such a standard receiver, the available correlator outputs are located at -0.25, 0 and 0.25 on the correlation function. The simple ratio with $X = 0.25$ and $Y = 0$ is formed. Figure 5 illustrates the lack of correlation between the raw value of the metric and the code pseudorange error. The coefficient of correlation between the two variables is -0.19. Values of errors up to 8 meters are not detected. The correlator outputs are low pass filtered with a rectangular low pass filter with 3Hz noise equivalent bandwidth. The narrowness of the low pass filter bandwidth is limited by the coherence time of the multipath, which in turn depends on the dynamic of the vehicle. The metric formed after filtering is shifted by a constant delay that maximizes the correlation between the metric and the code pseudorange error (e.g. 0.16 seconds for 3 Hz filtering). Figure 6 illustrates the existing correlation between the value of the metric and the code pseudorange error. The scatter is characteristic of two correlated variables. The magnitude of the coefficient of correlation between both variables is improved to -0.53. For a fixed maximum tolerable error and

$P_{fa}(m_{exp} = 2)$, the P_{MD} has decreased according to Figure 6. It reflects an improvement of sensitivity. Largest code errors are located in the right bottom region in Figure 4, which corresponds to a successful detection of abnormal error. Table 7 contains the P_{FA} and P_{MD} as functions of the expansion factor chosen to set the thresholds. Firstly, Table 7 shows that the observed P_{FA} in urban environment is lower than the expected P_{FA} . In presence of several reflections and due to their impact on tracking loops, the distribution of the metric is different. New thresholds could be derived from these simulations to force the P_{FA} to the expected value, based on gaussianity assumption and by measuring the standard deviation of the metric. However, the validity of these thresholds would rely on too many hypotheses such as the satellite elevation, the loop bandwidths, the chip spacing and the vehicle dynamic to name a few. Table 7 also proves the major improvement obtained by smoothing the correlator outputs. Indeed for every expansion factor, the P_{FA} and P_{MD} are lower after low pass filtering. Anyway, in this set of simulations, the magnitudes of the pseudorange errors are not large enough to be detected when setting a low P_{FA} (e.g. $m_{exp} = 3$).

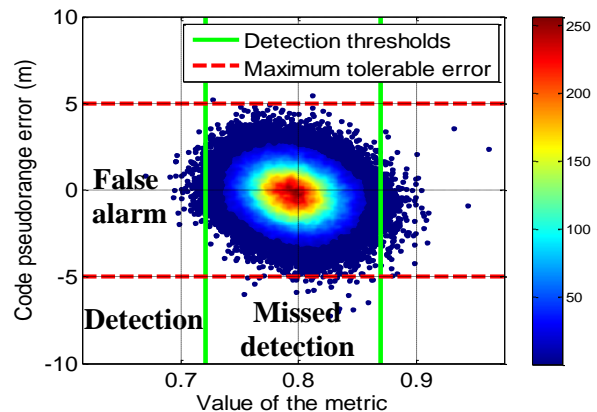


Figure 5 Correlation between code pseudorange error and value of the raw simple ratio metric (M_1) for BPSK

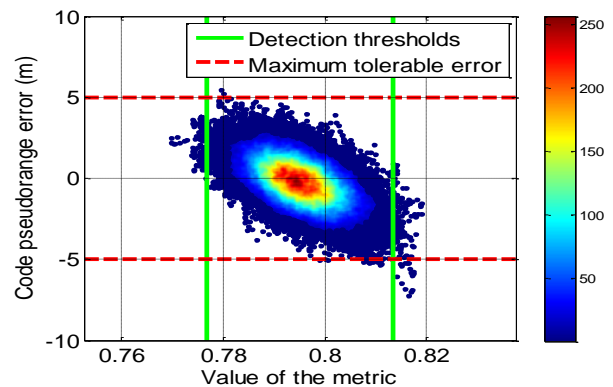


Figure 6 Correlation between code pseudorange error and value of the simple ratio metric (M_1) after smoothing the correlator outputs for BPSK

Theoretical P_{FA}	0.027	0.046	0.072	0.11	0.16
P_{FA} w/o filtering	0.0045	0.0088	0.018	0.034	0.063
P_{MD} w/o filtering	1	1	0.88	0.88	0.79
P_{FA} w/ filtering	0.0028	0.0056	0.0129	0.027	0.051
P_{MD} w/ filtering	0.52	0.52	0.30	0.17	0.090

Table 7 Performances of the test based on the simple ratio test

Performance comparison with C/N_0 estimator

A conventional way for the receivers to monitor the signal quality is to estimate the C/N_0 . The objective is here to compare the ability of the C/N_0 estimation to detect error with high magnitude with the ability of a test based on the distortion metrics.

The C/N_0 estimator used is:

$$\widehat{C/N_0} = A - 1 + \sqrt{A(A - 1)} \quad (13)$$

Where:

$$A = \frac{E[I_p^2 + Q_p^2]^2}{\text{var}(I_p^2 + Q_p^2)} \quad (14)$$

The expectation and the variance are estimated over 1 second. We firstly compare the behavior of this estimator in presence of a 40 dB-Hz noise, with and without multipath.

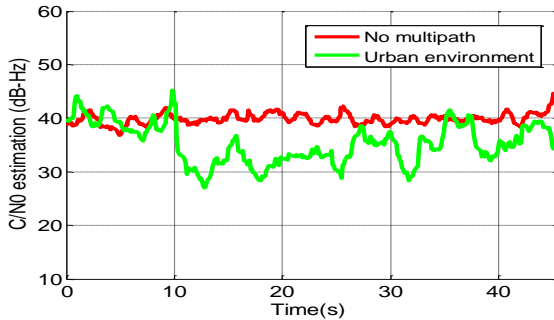


Figure 7 Estimation of C/N_0 with true C/N_0 set to 40dB-Hz

The quality of the C/N_0 estimation is degraded by the presence of multipath according to Figure 7. As the C/N_0 is used for the determination of the detection threshold of the metric (in the expression of μ). A possible solution is to smooth the C/N_0 estimate [5]. Moreover, it has already been proven that the Signal to Noise Ratio (SNR) error is correlated (and in phase) with the multipath delay error [14]. This phenomenon can be illustrated through the simulation platform by processing the LMS output without adding any thermal noise. The shape of the scatter in Figure 8 shows that the highest multipath error occurs for low estimated C/N_0 . It is therefore relevant to define a

monitoring algorithm based on this detector and it is then necessary to set the lower bound for the detector. A typical value is 30 dB-Hz [9] because it is a good trade-off between NLOS exclusion and availability. The efficiency of this monitoring approach is assessed on the LMS and affected by a 40 dB-Hz thermal noise. The code pseudorange error is plotted as a function of the estimated C/N_0 in Figure 9. Table 8 summarizes the performance of the C/N_0 based detection test for several threshold candidates. SNR monitoring outperforms the test based on raw metric monitoring. Indeed as an example for a P_{FA} of 0.019, the SNR monitoring has a P_{MD} of 47% whereas the raw metric performs a P_{MD} of 88%. On the other hand the detection power of the metric obtain after correlator smoothing is higher than the SNR test. For an expansion factor of 1.4, the P_{FA} is -6.3% which is lower than the P_{FA} of SNR with a threshold of 32 dB-Hz. Moreover the P_{MD} is 9% which outperforms the 33% obtained with the monitoring of the C/N_0 .

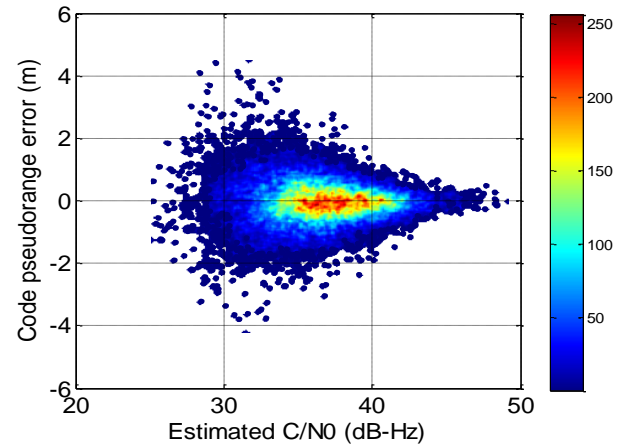


Figure 8 Correlation between code pseudorange error and estimated C/N_0 with multipath only for BPSK

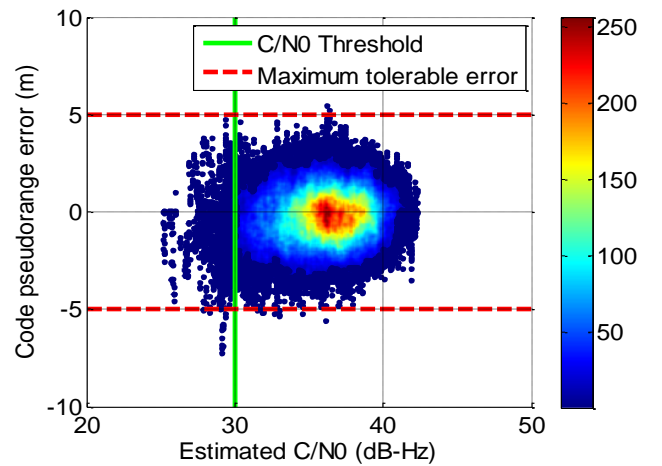


Figure 9 Correlation between code pseudorange error and estimated C/N_0 with multipath only for BPSK

C/N_0 (dB-Hz)	28	29	30	31	32
P_{FA}	0.0036	0.0080	0.019	0.043	0.083
P_{MD}	0.93	0.90	0.47	0.43	0.33

Table 8 Performance of the SNR monitoring

Other metrics

The same simulations were conducted for a differential ratio and non-coherent simple ratio. The differential ratio was formed by using $X = 0.25$ $Y = -0.25$ and $Z = 0$. This metric characterizes well the asymmetry of the correlation function. The correlation coefficient between the code error and this metric is 0.64 which is higher than the simple ratio metric. Table 9 summarizes the performance of this detector. No major improvement is obtained for the differential ratio compared to the simple ratio metric. Moreover the comparison in term of performance is difficult as the observed P_{FA} are not the same for both tests.

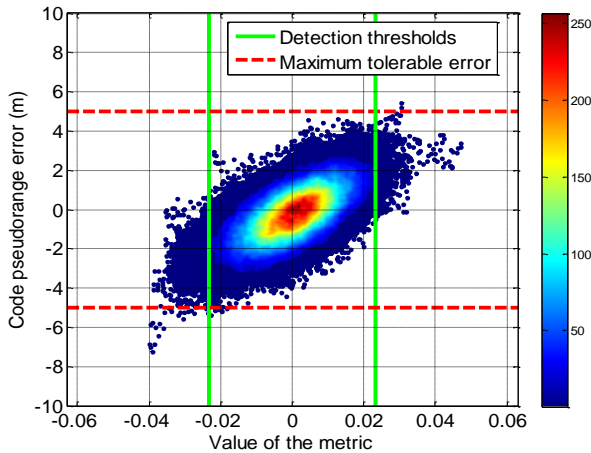


Figure 10 Correlation between code pseudorange error and differential ratio metric (M_2)

Theoretical P_{FA}	0.027	0.046	0.072	0.11	0.16
P_{FA}	0.007	0.012	0.023	0.040	0.069
P_{MD}	0.36	0.30	0.24	0.091	0.0

Table 9 P_{FA} and P_{MD} performed by monitoring the differential ratio metric

Finally a simple ratio non coherent test metric was implemented on the model of narrowband receiver, but the 3rd order PLL is replaced by a second order FLL with a 5 Hz loop bandwidth. The estimation of the frequency error is based on the non-coherent differential arctangent discriminator. The metric is formed with $X = 0.25$ and

$Y = 0$. The detection thresholds were determined a priori by simulating correlator output affected by thermal noise only. The results obtained in term of P_{FA} and P_{MD} are given in Table 10. Overall the performances of M_3 ratio are similar to the performances of M_1 and M_2 . It is therefore possible to implement a metric based test to detect the presence of multipath in a receiver using a FLL.

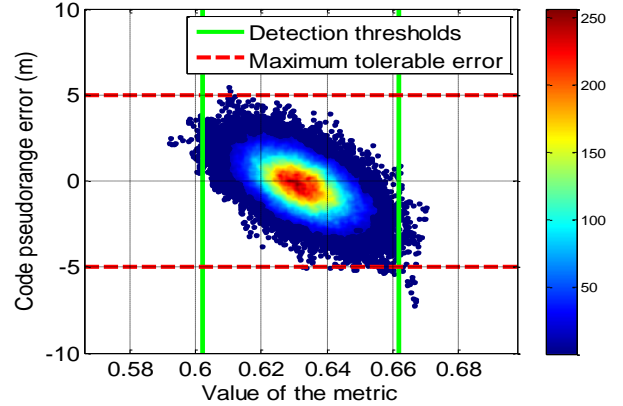


Figure 11 Correlation between code pseudorange error and non coherent simple ratio metric (M_3)

Theoretical	0.027	0.046	0.072	0.11	0.16
P_{FA}	0.002	0.0054	0.012	0.025	0.047
P_{MD}	0.63	0.52	0.30	0.21	0.18

Table 10 P_{FA} and P_{MD} performed by monitoring the non coherent simple ratio metric

BOC(1,1) signal

The simple ratio metric is tested with BOC(1,1) modulation with $X = 0.25$ and $Y = 0$. The location of Y is chosen in the validity domain according to Figure 1. Firstly, it can be inferred from Figure 11 that the magnitude of the pseudorange errors is lower for the BOC(1,1) modulation than BPSK. The maximum error does not reach 5 meters for BOC(1,1), therefore the maximum tolerable error is reduced to 3.5 meters. Table 10 shows that the metric is able to detect large errors even for BOC(1,1). Again, the errors observed do not have a sufficient amplitude to assess the performances for very low P_{FA} .

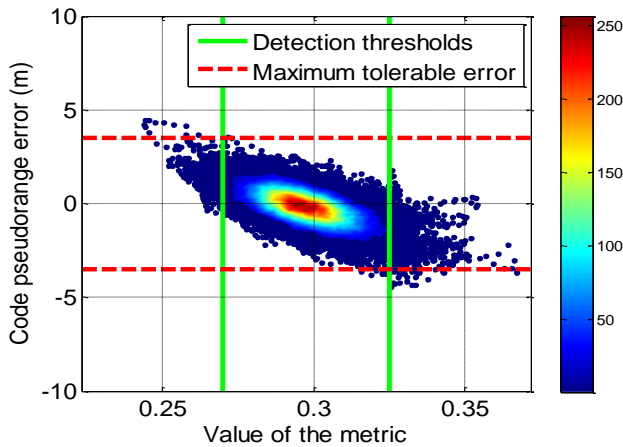


Figure 12 Correlation between code pseudorange error and simple ratio metric for BOC(1,1) modulation

Theoretical P_{FA}	0.027	0.046	0.072	0.11	0.16
P_{FA}	0.013	0.023	0.036	0.059	0.092
P_{MD}	0.32	0.18	0.054	0.036	0.018

Table 11 Performances of the simple ratio metric for BOC(1,1)

Future work

The processing of the LMS does not generate code error with amplitude of several tenth of meter when the received signal is the sum of a LOS signal and reflections. This phenomenon is partly due to the low probability to receive multipath with large or medium delays that generate large errors. Moreover the lifespan of the reflections do not exceed few seconds. Finally, the filtering effect of the multipath by the carrier loop because of the difference of Doppler frequency between the direct signal and the reflections also reduce the magnitude of the multipath error. Further work will focus on the testing of the multipath monitoring indicators on actual measurements in urban environment. The ability of the test to detect multipath error with large magnitude will be tested. Future work will also be conducted in order to consider the nominal distortion of the correlation due to other phenomenons such as evil-waveform in order to refine the detection thresholds.

Conclusion

This paper discussed the theoretical and simulated performance of a detection test based on correlation function distortion metrics. A new rigorous approach for the setting of the detection threshold is proposed. These thresholds enable to set the P_{FA} with a wider domain of validity. The sensitivity of the test is defined as the minimum SMR at which the test is able to detect the multipath with a fixed P_{MD} . It is then possible to theoretically assess the performances of the test metrics. It was proven in the paper that a detector formed with the

raw correlator outputs does not perform sufficiently in term of sensitivity. However, smoothing either the correlator outputs or the metric enable to narrow the confidence interval and therefore to significantly improve the sensitivity of the test. This improvement in term of SMR was quantized to 11 dB on a typical scenario. Finally the performances of the detector were assessed by simulation on a Land Mobile Satellite channel simulator coupled with a realistic GNSS receiver simulator. The correlation between the raw metric is low and therefore as expected the performance of such test are low. As theoretically proven, the smoothing of the correlator outputs highly improve the sensitivity of the test provided that the bandwidth of the filter is sufficiently high not to filter out the dynamic of the multipath. The performances of these tests were compared with a multipath detector based on the SNR estimation. Even if the SNR estimation shows promising detection abilities, the test based on filtered correlator outputs is more efficient to detect abnormally large code error. Finally similar performances were obtained for other existing and proposed metrics and other signals.

ACKNOWLEDGMENTS

This study was funded by the European GNSS Agency (GSA) as a part of the GENIUS project, Ecole Nationale de l'Aviation Civile (ENAC) and Egis.

REFERENCES

- [1] Van Dierendonck, A.J., P. Fenton and T. Ford (1992), Theory and Performance of Narrow Correlator Technology in GPS Receiver, NAVIGATION: Journal of The Institute of Navigation, Vol. 39, No.3, pp. 265-283
- [2] McGraw, Gary A., Braasch, Michael S., "GNSS Multipath Mitigation Using Gated and High Resolution Correlator Concepts," Proceedings of the 1999 National Technical Meeting of The Institute of Navigation, San Diego, CA, January 1999, pp. 333-342
- [3] Meguro, J., Murata, T., Takiguchi, J.-I., Amano, Y. and Hashizume, T. (2009). GPS Multipath Mitigation for Urban Area Using Omnidirectional Infrared Camera. IEEE Transactions on Intelligent Transportation Systems, Vol. 10, No. 1, 22 - 30
- [4] Phelts, R. E. (2001). Multicorrelator techniques for robust mitigation of threats to GPS signal quality (Doctoral dissertation, Stanford University).
- [5] Irsigler, Markus, Hein, Guenter W., "Development of a Real-Time Multipath Monitor Based on Multi-Correlator Observations," Proceedings of the 18th International Technical Meeting of the Satellite Division of The Institute of Navigation (ION GNSS 2005), Long Beach, CA, September 2005, pp. 2626-2637.
- [6] Sleewaegen, Jean Marie, Boon, Frank, "Mitigating Short-Delay Multipath: a Promising New Technique," Proceedings of the 14th International Technical Meeting of the Satellite Division of The Institute of Navigation (ION GPS 2001), Salt Lake City, UT, September 2001, pp. 204-213.
- [7] R. C. Geary, "The Frequency Distribution of the Quotient of Two Normal Variates", Journal of the Royal Statistical Society Vol. 93, No. 3 (1930) , pp. 442-446
- [8] D. V. Hinkley, "On the Ratio of Two Correlated Normal Random Variables", Biometrika, Vol. 56, No. 3 (Dec., 1969), pp. 635-639

- [9] Brocard, P.; Salos, D.; Julien, O.; Mabillean, M., "Performance evaluation of multipath mitigation techniques for critical urban applications based on a land mobile satellite channel model," *Position, Location and Navigation Symposium - PLANS 2014, 2014 IEEE/ION*, vol., no., pp.612,625, 5-8 May 2014
- [10] W. G. Bulgren, "On Representations of the Doubly Non-Central F Distribution", Vol. 66, No. 333 (Mar., 1971), pp. 184-186.
- [11] Scheffé, H. (1959). "The Analysis of Variance". John Wiley, New York
- [12] Lehner, Andreas, Steingass, Alexander, "A Novel Channel Model for Land Mobile Satellite Navigation," Proceedings of the 18th International Technical Meeting of the Satellite Division of The Institute of Navigation (ION GNSS 2005), Long Beach, CA, September 2005, pp. 2132-2138.
- [13] Prieto-Cerdeira, R., Perez-Fontan, F., Burzigotti, P., Bolea-Alamañac, A. and Sanchez-Lago, I. (2010), Versatile two-state land mobile satellite channel model with first application to DVB-SH analysis. *Int. J. Satell. Commun. Network.*, 28:, no 5-6, pp. 291-315, 2010.
- [14] Sleewaegen, Jean-Marie, "Multipath Mitigation, Benefits from using the Signal-to-Noise Ratio," *Proceedings of the 10th International Technical Meeting of the Satellite Division of The Institute of Navigation (ION GPS 1997)*, Kansas City, MO, September 1997, pp. 531-540.

APPENDIX

This appendix provides the proofs for the formulas that are used in the paper for the determination of the thresholds and the calculation of the sensitivity.

I. Determination of detection thresholds with gaussianity assumption

Simple ratio metric

In order to calculate the standard deviation of the simple ratio metric, the first order development in Taylor series gives:

$$\frac{I_X}{I_Y} = \frac{\mu_X + n_X}{\mu_Y + n_Y} \approx \frac{\mu_X + n_X}{\mu_Y} \left(1 - \frac{n_Y}{\mu_Y} + \left(\frac{n_Y}{\mu_Y} \right)^2 \right)$$

At the second order (the zero means and higher order terms are not written):

$$E \left[\frac{I_X^2}{I_Y^2} \right] = \frac{1}{\mu_Y^2} E \left[\mu_X^2 + n_X^2 - 4 \frac{\mu_X}{\mu_Y} n_Y n_X + 3 \frac{\mu_X^2}{\mu_Y^2} n_Y^2 \right]$$

We also have:

$$E \left[\frac{I_X}{I_Y} \right] = \frac{\mu_X}{\mu_Y} - \frac{1}{\mu_Y^2} E[n_X n_Y] + \frac{\mu_X}{\mu_Y^3} E[n_Y^2]$$

Finally

$$\sigma^2 \left(\frac{I_X}{I_Y} \right) = E \left[\frac{I_X^2}{I_Y^2} \right] - E \left[\frac{I_X}{I_Y} \right]^2$$

Thus

$$\sigma^2 \left(\frac{I_X}{I_Y} \right) = \left(\frac{\mu_X}{\mu_Y} \right)^2 \left(\frac{\sigma^2(n_X)}{\mu_X^2} + \frac{\sigma^2(n_Y)}{\mu_Y^2} - 2 \frac{\text{cov}(n_X n_Y)}{\mu_X \mu_Y} \right)$$

Differential ratio metric

In order to calculate the standard deviation of the differential ratio metric, the first order development in Taylor series gives:

$$\frac{I_X - I_Y}{I_Z} = \left(\frac{\mu_X + n_X - \mu_Y - n_Y}{\mu_Z} \right) \left(1 - \frac{n_Z}{\mu_Z} + \left(\frac{n_Z}{\mu_Z} \right)^2 \right)$$

$$E \left[\left(\frac{I_X - I_Y}{I_Z} \right)^2 \right] = E \left[\frac{I_X^2}{I_Z^2} + \frac{I_Y^2}{I_Z^2} - 2 \frac{I_X I_Y}{I_Z^2} \right]$$

The previous results can be used:

$$E \left[\frac{I_X^2}{I_Z^2} \right] = \frac{1}{\mu_Z^2} E \left[\mu_X^2 + n_X^2 - 4 \frac{\mu_X}{\mu_Z} n_Z n_X + 3 \frac{\mu_X^2}{\mu_Z^2} n_Z^2 \right]$$

$$E \left[\frac{I_Y^2}{I_Z^2} \right] = \frac{1}{\mu_Z^2} E \left[\mu_Y^2 + n_Y^2 - 4 \frac{\mu_Y}{\mu_Z} n_Z n_Y + 3 \frac{\mu_Y^2}{\mu_Z^2} n_Z^2 \right]$$

$$E \left[\frac{I_X I_Y}{I_Z^2} \right] = \frac{1}{\mu_Z^2} E \left[\mu_X \mu_Y + n_X n_Y - 2 n_Z n_Y \frac{\mu_X}{\mu_Z} - 2 n_Z n_X \frac{\mu_Y}{\mu_Z} + 3 n_Z^2 \frac{\mu_X \mu_Y}{\mu_Z^2} \right]$$

Moreover

$$E \left[\frac{I_X - I_Y}{I_Z} \right] = \frac{1}{\mu_Z} E \left[\mu_X - \mu_Y - n_Z n_X \frac{1}{\mu_Z} + n_Z n_Y \frac{1}{\mu_Z} + n_Z^2 \frac{\mu_X - \mu_Y}{\mu_Z^2} \right]$$

The 4th and 3rd order terms are not written:

$$E \left[\frac{I_X - I_Y}{I_Z} \right]^2 = \frac{1}{\mu_Z^2} \left[(\mu_X - \mu_Y)^2 + E[n_Z n_Y]^2 \frac{1}{\mu_Z} + 2 \frac{(\mu_X - \mu_Y)}{\mu_Z} (E[n_Z n_Y] - E[n_Z n_X]) + 2E[n_Z^2] \frac{(\mu_X - \mu_Y)^2}{\mu_Z^2} \right]$$

Then

$$\sigma^2 \left(\frac{I_X - I_Y}{I_Z} \right) = \frac{1}{\mu_Z^2} \left\{ \mu_X^2 + E[n_X^2] - 4 \frac{\mu_X}{\mu_Z} E[n_Z n_X] + 3 \frac{\mu_X^2}{\mu_Z^2} E[n_Z^2] + \mu_Y^2 + E[n_Y^2] - 4 \frac{\mu_Y}{\mu_Z} E[n_Z n_Y] + 3 \frac{\mu_Y^2}{\mu_Z^2} E[n_Z^2] - 2 \left[\mu_X \mu_Y + E[n_X n_Y] - 2E[n_Z n_Y] \frac{\mu_X}{\mu_Z} - 2E[n_Z n_X] \frac{\mu_Y}{\mu_Z} + 3E[n_Z^2] \frac{\mu_X \mu_Y}{\mu_Z^2} \right] - \left[(\mu_X - \mu_Y)^2 + 2 \frac{(\mu_X - \mu_Y)}{\mu_Z} (E[n_Z n_Y] - E[n_Z n_X]) + 2E[n_Z^2] \frac{(\mu_X - \mu_Y)^2}{\mu_Z^2} \right] \right\}$$

If X and Y do not have the same value:

$$\sigma^2 \left(\frac{I_X - I_Y}{I_Z} \right) = \left(\frac{\mu_X - \mu_Y}{\mu_Z} \right)^2 \left[\frac{\sigma^2(n_Z)}{\mu_Z^2} + \frac{\sigma^2(n_X) + \sigma^2(n_Y) - 2\text{cov}(n_X n_Y)}{(\mu_X - \mu_Y)^2} + 2 \left(\frac{\text{cov}(n_Z n_X) - \text{cov}(n_Z n_Y)}{\mu_Z (\mu_X - \mu_Y)} \right) \right]$$

II. Determination of detection thresholds with rigorous approach

Simple ratio metric

The expression of the Geary-Hinkley transform applied to $M = \frac{I_X}{I_Y}$ is the following:

$$\left| \frac{\mu_Y M - \mu_X}{\sqrt{\sigma_Y^2 M^2 - 2\text{cov}_{XY} M + \sigma_X^2}} \right| \leq m_{exp}$$

Which is equivalent to

$$M^2 (\mu_Y^2 - m_{exp}^2 \sigma_Y^2) + M (-2\mu_X \mu_Y + 2m_{exp}^2 \text{cov}_{XY}) + \mu_X^2 - m_{exp}^2 \sigma_X^2 \leq 0$$

The expression is always positive except between the roots of the polynomial then:

Lowerbound

$$= \frac{-(-2\mu_X\mu_Y + 2m_{exp}^2 cov_{XY}) - \sqrt{(-2\mu_X\mu_Y + 2m_{exp}^2 cov_{XY})^2 - 4(\mu_Y^2 - m_{exp}^2\sigma_Y^2)(\mu_X^2 - m_{exp}^2\sigma_X^2)}}{2(\mu_Y^2 - m_{exp}^2\sigma_Y^2)}$$

Upperbound

$$= \frac{-(-2\mu_X\mu_Y + 2m_{exp}^2 cov_{XY}) + \sqrt{(-2\mu_X\mu_Y + 2m_{exp}^2 cov_{XY})^2 - 4(\mu_Y^2 - m_{exp}^2\sigma_Y^2)(\mu_X^2 - m_{exp}^2\sigma_X^2)}}{2(\mu_Y^2 - m_{exp}^2\sigma_Y^2)}$$

Differential ratio metric

The expression of the threshold for the differential metric is derived from the thresholds of the simple ratio test.

III. Determination of the sensitivity

Simple ratio metric

The bounds of the biased distribution can be found the same way as they were found to set the P_{FA} . Here the P_{FA} is replaced by the P_{MD} .

The new distribution is bounded (with P_{MD}) between *Lowerbound, MP* and *Upperbound, MP*.

These can be obtained with the Geary-Hinkley transformation.

$$\mu_{X,MP} = \mu_X + \alpha K_{cc}(X - \tau)$$

$$\mu_{Y,MP} = \mu_Y + \alpha K_{cc}(Y - \tau)$$

The bounds of the confidence interval of the metric affected by multipath become:

$$\text{Lowerbound, MP} = \frac{-(-2\mu_{X,MP}\mu_{Y,MP} + 2m_{MD}^2 cov_{XY}) - \sqrt{(2\mu_{X,MP}\mu_{Y,MP} - 2m_{MD}^2 cov_{XY})^2 - 4(\mu_{Y,MP}^2 - m_{MD}^2\sigma_Y^2)(\mu_{X,MP}^2 - m_{MD}^2\sigma_X^2)}}{2(\mu_{Y,MP}^2 - m_{MD}^2\sigma_Y^2)}$$

$$\text{Upperbound, MP} = \frac{-(-2\mu_{X,MP}\mu_{Y,MP} + 2m_{MD}^2 cov_{XY}) + \sqrt{(2\mu_{X,MP}\mu_{Y,MP} - 2m_{MD}^2 cov_{XY})^2 - 4(\mu_{Y,MP}^2 - m_{MD}^2\sigma_Y^2)(\mu_{X,MP}^2 - m_{MD}^2\sigma_X^2)}}{2(\mu_{Y,MP}^2 - m_{MD}^2\sigma_Y^2)}$$

Then two configurations described in Chapter IV are possible.

Configuration 1:

$$\text{Lowerbound, MP} = UB_{\bar{M}P}$$

Where $UB_{\bar{M}P}$ is the upper detection threshold set in order to set the P_{FA} .

Then:

$$(-2\mu_{X,MP}\mu_{Y,MP} + 2m_{MD}^2 cov_{XY})^2 - 4(\mu_{Y,MP}^2 - m_{MD}^2\sigma_Y^2)(\mu_{X,MP}^2 - m_{MD}^2\sigma_X^2) = [-(-2\mu_{X,MP}\mu_{Y,MP} + 2m_{MD}^2 cov_{XY}) - 2UB_{\bar{M}P}(\mu_{Y,MP}^2 - m_{MD}^2\sigma_Y^2)]^2$$

After transformation transformations it becomes:

$$\begin{aligned} & UB_{\bar{M}P}^2 (\mu_{Y,MP}^2 - m_{MD}^2\sigma_Y^2) \\ & + UB_{\bar{M}P} (-2\mu_{X,MP}\mu_{Y,MP} \\ & + 2m_{MD}^2 cov_{XY}) + (\mu_X^2 - m_{MD}^2\sigma_X^2) \\ & = 0 \end{aligned}$$

The unknown is α , and after replacing $\mu_{X,MP}$ and $\mu_{Y,MP}$ by their expressions in function of α the equation becomes:

$$\begin{aligned} & \alpha^2 \{ [UB_{\bar{M}P} K_{cc}(Y - \tau)]^2 \\ & - 2UB_{\bar{M}P} K_{cc}(Y - \tau) K_{cc}(X - \tau) \\ & + K_{cc}(X - \tau)^2 \} \\ & + \alpha \{ 2UB_{\bar{M}P}^2 \mu_Y K_{cc}(Y - \tau) \\ & - 2UB_{\bar{M}P} [\mu_X K_{cc}(Y - \tau) \\ & + \mu_Y K_{cc}(X - \tau)] + 2\mu_X K_{cc}(X - \tau) \} \\ & + UB_{\bar{M}P}^2 (\mu_Y^2 - m_{MD}^2\sigma_Y^2) \\ & + 2UB_{\bar{M}P} (-\mu_X\mu_Y + m_{MD}^2 cov_{XY}) + \mu_X^2 \\ & - m_{MD}^2\sigma_X^2 = 0 \end{aligned}$$

The lowest root of this equation is the sensitivity associated with the probability of missed detection m_{MD} .

Configuration 2:

$$\text{Upperbound, MP} = LB_{\bar{M}P}$$

Where $UB_{\bar{M}P}$ is the upper detection threshold set in order to set the P_{FA} .

$$\begin{aligned} & \alpha^2 \{ [LB_{\bar{M}P} K_{cc}(Y - \tau)]^2 - 2LB_{\bar{M}P} K_{cc}(Y - \tau) K_{cc}(X - \tau) \\ & + K_{cc}(X - \tau)^2 \} \\ & + \alpha \{ 2LB_{\bar{M}P}^2 \mu_Y K_{cc}(Y - \tau) \\ & - 2LB_{\bar{M}P} [\mu_X K_{cc}(Y - \tau) \\ & + \mu_Y K_{cc}(X - \tau)] + 2\mu_X K_{cc}(X - \tau) \} \\ & + LB_{\bar{M}P}^2 (\mu_Y^2 - m_{MD}^2\sigma_Y^2) \\ & + 2LB_{\bar{M}P} (-\mu_X\mu_Y + m_{MD}^2 cov_{XY}) + \mu_X^2 \\ & - m_{MD}^2\sigma_X^2 = 0 \end{aligned}$$

The lowest root of this 2nd order equation is the sensitivity associated with the probability of missed detection Th_{MD} .

Differential ratio metric

Substitute X by N , and Y by Z in the general expression